



Published in final edited form as:

*J Comp Neurol.* 2005 August 1; 488(3): 255–268.

## Octopamine-Immunoreactive Neurons in the Brain and Subesophageal Ganglion of the Hawkmoth *Manduca sexta*

A.M. Dacks<sup>1</sup>, T.A. Christensen<sup>1,\*</sup>, H.-J. Agricola<sup>2</sup>, L. Wollweber<sup>3</sup>, and J.G. Hildebrand<sup>1</sup>

1. Arizona Research Laboratories, Division of Neurobiology, University of Arizona, P. O. Box 210077, Tucson, AZ 85721-0077

2. Friedrich-Schiller-Universität Jena, Institut für Allgemeine Zoologie und Tierphysiologie, Erbertstraße 1, 07743 Jena, Federal Republic of Germany

3. Institut für Molekulare Biotechnologie, Beutenbergstraße 11, 07745 Jena, Federal Republic of Germany

### Abstract

Octopamine is a neuroactive monoamine that functions as a neurohormone, a neuromodulator and a neurotransmitter in many invertebrate nervous systems, but little is known about the distribution of octopamine in the brain. We therefore used a monoclonal antibody to study the distribution of octopamine-like immunoreactivity in the brain of the hawkmoth *Manduca sexta*. Immunoreactive processes were observed in many regions of the brain, with the distinct exception of the upper division of the central body. We focused our analysis on nine ventral unpaired median (VUM) neurons with cell bodies in the labial neuromere of the subesophageal ganglion. Seven of these neurons projected caudally through the ventral nerve cord. Two neurons projected rostrally into the brain (supraesophageal ganglion), and one of these was a bilateral neuron that sent projections to the  $\gamma$ -lobe of the mushroom body and the lateral protocerebrum. Octopamine-immunoreactive processes from one or more cells originating in the subesophageal ganglion also form direct connections between the antennal lobes and the calyces of the mushroom bodies.

### Keywords

insect brain; learning; neuromodulation; octopamine; olfaction; VUM

### Introduction

Octopamine (OA), a structural analog of norepinephrine, is one of the most extensively studied biogenic amines in the nervous system of many invertebrates. Over the past several decades, accumulating evidence has shown that OA can function as a neurohormone, neuromodulator, and as a classical neurotransmitter. In insects, it plays important roles in diverse behaviors from flight metabolism (Orchard and Lange, 1984) and visual dishabituation in locusts (Stern, 1999), to bioluminescence in fireflies (Christensen et al., 1983). Most contemporary accounts describe OA as an important mediator of “fight or flight” responses (for an extensive review, see Roeder, 1999), but it also may play key roles in higher behavioral functions, such as olfactory learning (Mercer and Menzel, 1982; Dudai et al., 1987; Hammer, 1993; Kreissl et al., 1994; Hammer and Menzel, 1995; Hammer and Menzel, 1998; Farooqui et al., 2003; Schwaerzel et al. 2003). In honey bees and fruitflies, blocking the actions of OA in the antennal lobes (ALs) or the mushroom bodies (MBs) by pharmacological or molecular means impairs appetitive olfactory learning (Dudai et al., 1987; Farooqui et al., 2003; Schwaerzel et al.

\*To whom correspondence should be addressed. E-mail: tc@neurobio.arizona.edu.

2003). Furthermore, injection of OA into the ALs and MBs can rescue or enhance learned responses (Mercer and Menzel, 1982; Menzel et al., 1999), and it can also substitute for the unconditioned stimulus (US) during olfactory conditioning (Hammer and Menzel, 1998). A possible source of OA in the ALs and MBs of the honey bee is the VUMmx1 neuron, which has widespread bilateral projections in the ALs, MBs and lateral protocerebrum, and signals the presence of the US (Hammer, 1993, Hammer and Menzel, 1995).

To our knowledge, there have been no detailed neuroanatomical studies of OA like immunoreactivity (OAir) in Lepidoptera (e.g. see Homberg, 1994), but numerous studies in several moth species have demonstrated that OA has a number of different behavioral and physiological effects. For example, OA modulates the activity of olfactory receptor neurons (Pophof, 2000; Dolzer et al., 2001; Grosmaître et al., 2001; Pophof, 2002; Stelinski et al., 2003), it increases the sensitivity of male moths to female sex pheromone (Linn and Roelofs, 1986; Linn et al., 1992), and it modulates the activity of flight motor neurons (Claassen and Kammer, 1986; Fitch and Kammer, 1986; Klaassen et al., 1986). More recently, it has been demonstrated that moths are also excellent models for studies of olfactory-based appetitive learning (Hartlieb, 1996; Fan et al., 1997; Hartlieb et al., 1999; Daly and Smith, 2000; Daly et al., 2001a, b, 2004; Fan and Hansson, 2001; Cunningham et al., 2004), but the possible role of OA in moth olfactory learning remains unclear.

OA has been isolated from the brain of the hawkmoth *Manduca sexta* by means of HPLC (Davenport and Wright, 1986; Lehman et al., 2000b), and the development of putatively octopaminergic neurons in the abdominal ganglia of *M. sexta* has also been described (Pflüger et al., 1993; Lehman, et al., 2000a). Details of the distribution of OA in the brain, however, have yet to be described in any lepidopteran species. As a first step toward unraveling the possible role of OA in moth olfactory learning, we describe the distribution of OA-like immunoreactivity as well as the morphological details of Ventral Unpaired Median (VUM) neurons with cell bodies in the subesophageal ganglion (SEG) that send extensive projections to different areas of the brain involved in learning and memory. Where appropriate, we make comparisons to observations reported previously in other insect species.

## MATERIALS AND METHODS

### Animals

*M. sexta* (Lepidoptera: Sphingidae) were reared as larvae on artificial diet (modified from that of Bell and Joachim, 1976) and kept at 25° C and 50-60% relative humidity under a long-day photoperiod regimen (17:7h; L:D) as described previously (Christensen and Hildebrand, 1987). Both adult males and females, 2 days post-eclosion, were used in this study.

### Production of the monoclonal octopamine antibody MAb-OA1

Octopamine was coupled to thyroglobulin by means of glutaraldehyde (Muller, 1988). Briefly, 1 ml 2% (v/v) glutaraldehyde in phosphate-buffered saline (PBS), pH 7.4, was added with shaking to a solution of 1 mg D,L-octopamine hydrochloride (Aldrich) in 1 ml PBS. After 3 min at room temperature, the solution was added dropwise to a solution of 15 mg thyroglobulin (Sigma) in 1 ml PBS. The reaction was allowed to proceed for 45 min at room temperature and then stopped by addition of 300 µl of sodium borohydride (50 mg NaBH<sub>4</sub>/ml PBS). After 1 h at 4° C the solution was dialysed against PBS for 24 h at 4° C and stored in aliquots at -20° C. For ELISA, D,L-octopamine was coupled to poly-L-lysine according to the procedure described above. Poly-L-lysine hydrobromide (8 mg) in 1 ml PBS was used in experiments.

## Immunization

Female BALB/c mice (10-20 weeks old) were immunized subcutaneously with 60 µg of octopamine-thyroglobulin conjugate emulsified in Freund's complete adjuvant. Five weeks later, 100 µg conjugate in 200 µl of PBS was injected intraperitoneally. Injections were repeated four more times at 2-3-week intervals. The antisera were collected 7 days after the last injection and tested for determination of the antibody titer and specificity using ELISA and immunocytochemistry.

## Cell fusion and cell culture

Four days after the last immunization, the splenic cells of a mouse were fused with the P3X63-Ag8.653 myeloma cells (Kearny et al. 1979). 107 lymphocytes were fused with 107 myeloma cells by use of 42% polyethylene glycol 4000 (Merck) according to standard procedures (Harlow and Lane, 1988). The fused cells were distributed into five 96-well microculture plates over a feeder cell layer of mouse peritoneal cells, and selection for hybridoma growth was conducted in 5.8 µM azaserine and 0.1 mM hypoxanthine-containing RPMI 1640 medium supplemented with 20% fetal calf serum (Karsten and Rudolph, 1985). Cells grew in a 37° C humidified incubator with 5% CO<sub>2</sub> in air. After incubation for 7 days, the culture supernatant from each of the wells was assayed by ELISA using microtiter plates coated with octopamine-poly-L-lysine. Individual colonies of hybridomas in wells with specific antibody were isolated in fresh wells containing feeder cells by means of a plastic capillary connected with a syringe. After five cloning steps, the hybridomas were frozen and stored in liquid nitrogen or cultivated *in vivo* for production of monoclonal antibodies (MAbs).

## Preparation and purification of monoclonal octopamine antibody (MAB-OA1)

The hybridoma cells (106 cells/0.5 ml) were injected intraperitoneally into each female BALB/c mice that had been sensitized by an intraperitoneal injection of 0.3ml of pristane (Serva). After 2-3 weeks the ascites fluid was collected, centrifuged and stored at -20° C until used. For purification from the ascites fluid, MAb-OA1 was precipitated twice with ammonium sulfate (50% saturation) at 4° C following dialysis against PBS overnight.

## Isotyping

The subclass of the MAb was determined in an OA-poly-L-lysine-coated microtiter plate by means of goat anti-isotype antibodies (Sigma) and horseradish peroxidase-labeled rabbit anti-goat immunoglobulin conjugates (Essig, 1990). MAb-OA1 belongs to the IgG 2a subclass.

## Determination of cross-reactivity

An indirect competitive ELISA procedure was used as described by Murphy et al. (1992). Microtiter plates (Nunc MaxiSorp, F96) were coated with an octopamine-poly-L-lysine conjugate (100 µl/well, 20 µg/ml PBS) at 4° C overnight. The wells were washed three times with PBS, and the remaining sites for protein binding on the plate were blocked with PBS containing 2% (w/v) bovine serum albumin (BSA) and 0.05% (w/v) Tween 20 (blocking buffer) at room temperature (1 h). After rinsing with PBS containing 0.05 % Tween 20 (PBS-T), 100 µl of antigen solutions ranging in concentration from 0.39 µg/ml to 400 µg/ml pre-incubated with culture supernatant of MAb OA-1 for 1 h at room temperature per well were added. After 15 min the wells were washed with PBS-T and incubated with 100 µl of peroxidase-labeled goat anti-mouse immunoglobulin (Sigma, 1 h) diluted 1:4000 in PBS. The plates were washed again in 100 µl of a solution containing 10 mg of o-phenylenediamine (Sigma), and 5 µl 30% (w/w) H<sub>2</sub>O<sub>2</sub> in 10 ml of 50 mM phosphate/25 mM citrate buffer (pH 5.1) was added into each well. After a 30 min incubation at room temperature, the enzymatic reaction was stopped by addition of 50 µl sulphuric acid (2M). The plates were utilized on a microplate reader model 3550 (Bio-Rad) at a wavelength of 490 nm.

### Antibody specificity

To establish the specificity of MAb OA-1, we developed a highly sensitive indirect competitive enzyme-linked immunosorbent assay (ELISA). This qualitative and quantitative screening revealed that MAb OA-1 had high affinity to the tested OA-poly-L-lysine conjugate. Seven different biogenic amines ranging in concentration from 0.39 µg/ml to 400 µg/ml were tested for a possible inhibition to the high affinity reaction. The relative cross-reactivity (calculated by dividing the concentration of OA at 50% inhibition by the concentration of the cross-reacting substance at 50% inhibition x 100) was 100% to OA, 63% to epinephrine, 21% to tyramine and 8% to norepinephrine. Dopamine, DOPA, and serotonin showed 0% inhibition (Fig. 1). Importantly, either use of MAb OA-1 pre-absorbed with pure OA (100 µg/ml) or omission of the primary antibody resulted in absence of tissue staining. The labeling we report cannot represent norepinephrine or epinephrine staining as the brain of *M. sexta* lacks the ability to synthesize or store norepinephrine (Maxwell et al., 1978), the precursor for epinephrine. Thus, it is impossible for the staining described in this paper to depict labeling of either of these neurotransmitters, as neither of them is present in the nervous system. We do acknowledge, however, that some of the labeled neurons may contain tyramine and not OA.

### Technical considerations

The distribution of OA in invertebrate nervous systems has always been difficult to characterize because of the speed with which OA breaks down or is released from neurons before the tissue can be fixed (Evans, 1984; Davenport and Evans, 1984). Cellular projections may be too fine to visualize, may not uniformly contain OA, or may be only partially labeled. Because of these caveats, we do not claim that the processes visualized in this study represented the full extent of the octopamine-expressing network in *M. sexta*. The processes arising from OA cell bodies are described to the fullest extent possible, and otherwise, only the positions of the cell bodies are reported.

### Preparation of brain tissue

At approximately 4 h into photophase, animals were placed on ice to decrease the amount of OA released in response to stress (see Evans, 1984; Davenport and Evans, 1984). A total of 52 animals were used for this study. Brains were dissected and tracheae were removed in dissecting solution (0.1M sodium cacodylate, sodium metabisulfite (SMB) 10 g/l, pH 6.2). Brains were then placed in fixative solution (0.1 M sodium cacodylate, 2% paraformaldehyde, 1% glutaraldehyde) for 3 h and subsequently embedded in agarose and sectioned on a Vibratome (Technical Products International, St. Louis, MO) at 100 µm or 150 µm in Tris buffer with SMB (0.5 M Tris, SMB 8.5g/l, pH 7.5). Frontal, horizontal, and sagittal sections were cut in order to obtain the most complete reconstructions of the immunostained projections as possible. Sections were incubated at room temperature for 10 min in Tris SMB with 0.1M sodium borohydride and then washed five times for 15 min in Tris SMB at room temperature and incubated overnight at room temperature in Tris SMB containing 30% sucrose.

### Immunocytochemistry

The following day the sections were washed three times for 15 min in Tris SMB at room temperature and incubated for two days at 4° C in a blocking solution (Tris SMB with 0.25% TX100, 1% NGS, 0.25% BSA, 3% fat-free milk powder; Donini et al., 2001) containing a 1:1000 MAb OA-1. After two days, the sections were washed three times for 15 min at room temperature in Tris-buffered saline (0.5M Tris, sodium chloride 8.5 g/l, pH 7.5). The sections were then incubated overnight at room temperature in blocking solution containing 1:200 goat anti—mouse Alexa Fluor 546 as a secondary antibody (Molecular Probes, Inc., Eugene, OR). The following day, the sections were washed five times for 15 min in Tris-buffered saline, dehydrated, and rehydrated in ethanol (50%, 70%, 95%, 100%) in order to remove gas from

the tracheae within the tissue. The sections were then cleared in a glycerol series (40%, 60%, 80%) and mounted on slides. Control preparations in which the primary antibody was omitted from the protocol did not reveal any immunoreactive cell bodies or fibers (data not shown). Fluorescent images were viewed with a laser-scanning, confocal microscope (Nikon E 800 with Nikon PCM 2000) equipped with Green HeNe lasers and appropriate filters. Digitized optical sections were made at intervals of 2  $\mu\text{m}$  for 20X magnification and at 1  $\mu\text{m}$  for 40X and 60X magnifications through the depth studied. The digitized images were modified only to enhance contrast. Image processing and labeling were performed with Simple PCI (Compix, Inc., Cranberry Township, PA) and Corel Draw 9.0 (Corel Corp., Ottawa, Ontario, Canada).

### Definition of unpaired median neurons

It is tempting to classify any medially located neuron as an “unpaired median neuron.” In this manuscript we adhere to the classical definition of an unpaired neuron as one having a projection pattern that is bilaterally symmetrical, as first described by Hoyle (1975). The term “unpaired” in this case does not refer to the number of cell bodies present, but rather, to the nature of the projection pattern. Thus, unless we were able to determine that a medially located cell body produced bilaterally symmetrical projections, the cell body in question was not labeled as unpaired.

## RESULTS

We found approximately 70 octopamine-like immunoreactive (OAir) cell bodies distributed throughout the SEG and protocerebrum of *M. sexta*. Some OAir cell bodies were found in distinct clusters, whereas others occurred individually (Fig. 2). Here we describe the locations of the OAir cell bodies and (when possible) the major projections of these neurons. Fine OAir fibers were observed in almost all neuropil structures of the brain, and we could determine the origin of these fibers in many cases through careful reconstruction of serial confocal images.

### Ventral Unpaired Median (VUM) neurons

One median cluster of 9 OAir somata, each averaging ca. 16 $\mu\text{m}$  in diameter, was found in the ventral portion of the labial neuromere (based on descriptions of the SEG neuromeres by Davis et al., 1996) of the SEG (Fig. 3a, e). We base our nomenclature on established standards: given their bilaterally projecting branches (see below), we refer to these cells as VUM neurons (see Methods), and given their location in the labial neuromere, they are labeled as VUMIb neurons. Each VUMIb neuron was assigned a number based on its stereotyped projection pattern as observed across animals (described below).

Seven VUMIb neurons projected posteriorly in the SEG before bifurcating (Fig. 3b). Each neurite in this bundle divided in the dorso-posterior neuropil of the SEG (Fig. 3c), sending axon branches down each cervical connective in the VNC (Fig. 3d). These neurons were named VUMIb3-9 and the descending projections that they produced were not traced further in this study. Two additional VUMIb neurons (VUMIb1 and 2) projected anteriorly and then dorsally before bifurcating, sending one process anteriorly and the other posteriorly (Fig. 3e-g). Unlike VUMIb3-9, these two cells had projections that ascended into the protocerebrum (see below). Two additional, very weakly OAir neurons, the ventral SEG (VS) neurons, were located in the maxillary neuromere (Fig. 3h). These cells projected posteriorly and joined a loose bundle of projections from the dorsal SEG neurons (see below) (Fig. 3i). We do not refer to these neurons as “VUM” neurons, as it was unclear if their projections were bilateral (see Methods).

Of the two anteriorly projecting VUMIb neurons that were stained, we were able to reconstruct the morphological details of one of them in considerable detail. This neuron, named VUMIb1, projected anteriorly and dorsally before bifurcating (Figs. 4a-d) along the lateral axis of the



SEG. These second-order branches again bifurcated (Fig. 4e) before ascending from the SEG and passing between the protocerebral medulla cells (see below) and the esophageal foramen (Fig. 4f). These paired, parallel fibers on each side of the brain extended dorsally through the tritocerebrum (Fig. 4f inset) toward the dorsal protocerebrum. As these thick branches extended dorsally, they gave rise to thin collaterals that densely innervated the surface of the  $\gamma$ -lobe of the ipsilateral mushroom body (Figs. 4g, h). The paired, parallel fibers then continued dorsally and arborized extensively (Fig. 4i) throughout the dorsal protocerebrum (Fig. 4j). These arborizations extended mostly ipsilaterally (but one branch extended contralaterally; Fig. 4j) and ran along the dorsal-most margin of the protocerebrum, passing near the dorsal protocerebral neurons described below (Fig. 2b). Figure 4k is a schematic reconstruction illustrating the striking bilateral symmetry of the VUM1b1 neuron.

### Dorsal Subesophageal-ganglion (DS) neurons

We found approximately 12-14 OAir cell bodies, each ca. 19  $\mu\text{m}$  in diameter, spread across the dorsal surface of the SEG. These dorsal SEG (DS) cells were situated directly below the esophageal foramen (Figs. 2b; 5a, b), and the majority were in the posterior portion of the SEG near the point at which most of the bilateral VUM1b axons turned to project down the ventral nerve cord (Fig. 5b). Because of the density of OAir labeled processes in this region of neuropil, we were unable to confirm whether the DS neurons had bilaterally symmetrical projections, and thus could not identify them as dorsal unpaired median (DUM) neurons.

Several DS neurons projected ventrally for a short distance and then extended dorsally back toward the esophageal foramen, while others sent projections directly toward the tritocerebrum (Fig. 5a). The projections of the DS neurons ran along the ventral side of the esophageal foramen (Fig. 5c) before entering the tritocerebrum. The projections arborized first in the anterior portion of the tritocerebrum near the PM neurons (Fig. 5c, d), but also slightly more posteriorly (Fig. 5e). The projections extended into both the ventral and dorsal regions of the tritocerebrum, both above and below the bundle of neurites from the PM neurons (Fig. 5d, e). The processes of the two VS neurons appeared to intermingle with these processes, at least within the SEG (see above), which was a source of difficulty in reconstructing single DS neurons. It should be noted, however, that the projection patterns of the DS neurons beneath the esophageal foramen were remarkably similar to the projection patterns of DUM neurons in the locust metathoracic ganglion, which form a “deep DUM tract” in which processes dive into the SEG and make a hairpin turn before bifurcating, or a “superficial DUM tract” in which DUM neurons project along the ventral surface of the esophageal foramen before bifurcating (Watson, 1984).

### Projections innervating the ALs and MBs originating from the SEG

Three OAir processes innervated the ALs of *M. sexta*. We could not discern the origin of these fibers solely from the immunocytochemical staining, although the DS neurons and VUM1b2 are the most likely candidates. A set of paired projections ascended from each side of the dorsal SEG through the tritocerebrum (Figs. 6a, b) and each of the projections then divided along the longitudinal axis of the brain (Fig. 6a, b), sending one process into the AL (Fig. 6c), and the other process posteriorly along the inner antenno-cerebral tract into the protocerebrum (Fig. 6a). In addition, a third OAir process entered the AL (Fig. 6d) anterior to the pair of projections described above. The OAir processes converged in the coarse neuropil (Fig. 6e) and arborized into finely-branching fibers that innervated all of the AL glomeruli (Fig. 6f, g). None of the cell bodies from the lateral, medial, or anterior cell clusters of the AL were OAir. The second set of OAir processes that ran through the inner antenno-cerebral tract invaded the base of the mushroom body calyces, where they arborized extensively (Fig. 6i, j). Dense arborizations were also visible in both the primary and secondary pedunculi (Fig. 6j). A diagram

summarizing the morphology of the projections that interconnect the ALs and the MBs is shown in Figure 6k.

### Protocerebral Medulla (PM) neurons

Another cluster of cell bodies was situated on either side of the esophageal foramen. Each cluster contained nine OAir cell bodies, each ca. 20  $\mu\text{m}$  in diameter (Fig. 2a; 7a, b). These neurons projected posteriorly along the foramen in a bundle (Fig. 7c) to the ipsilateral protocerebrum and optic lobe (Fig. 7c, d). They were similar in number, size, position, and projection to a group of neurons previously described in the locust, the protocerebral medulla (PM) neurons (Bacon et al., 1995; Stern et al., 1995; Stern, 1999). Homologous neurons were first described in honey bees (Kreissl et al., 1994), and neurons with similar projection patterns also have been observed in several other insect species (Monastirioti et al., 1995; Sinakevitch et al., 2001).

### Dorsal Protocerebral (DP) neurons

There are approximately 10-12 OAir cell bodies in the dorso-posterior region of the protocerebrum (DP; Fig. 2b), two of which produced projections that demonstrated OAir (Fig. 8). One cell body on each side of the brain gave rise to a thick OAir process that extended ventrally and branched above the upper division of the central body, sending one branch anteriorly and another branch ventrally toward the SEG (Fig. 8).

### Additional OAir cell bodies

Several OAir cell bodies were labeled consistently in the same locations, but their processes were not immunoreactive (Fig. 9a). For example, there were three pairs of OAir cell bodies in the anterior region of the dorsal SEG (Fig. 2a; these should not be confused with the DS neurons in Figure 2b). In addition, a single OAir cell body was situated below each antennal lobe (Fig. 9b). This pair of cells occupied positions similar to those of a pair of OAir cell bodies described in both honey bees (Kreissl et al., 1994) and locusts (Stern et al., 1995). In the dorsal protocerebrum, most of the DP cells (with the two exceptions cited above) lacked OAir processes (Fig. 9c). We also found a pair of cell bodies in the ventral portion of the juncture between the optic lobe and the protocerebrum (Figs. 2b; 9d), dorso-lateral to the lateral optic foci (Strausfeld, 1976). The projections of the neurons extended dorso-medially and then turned sharply dorsally (Fig. 9d).

### Bilateral projections to SEG

A pair of OAir fibers (one in each cervical connective) entered the SEG from the ventral nerve cord (Fig. 10a) and extended into the mandibular neuromere before projecting dorsally (Fig. 10b) toward the mandibular commissure. At the mandibular neuromere, they bifurcated, and one branch remained in the ipsilateral neuropil while the other branch crossed the midline via the mandibular commissure to the contralateral side. The mirror-image of this branching pattern occurred in the fiber arising from the other connective (Fig. 10c) and as these two fibers crossed the midline they became intertwined (Fig. 10d). On the contralateral side, the crossing branch divided and produced fine arborizations in areas dorso-and ventro-lateral to the crossing branches (Fig. 10d).

## DISCUSSION

### Anatomy of OAir in the brain of *M. sexta*

We have identified several clusters of OAir cell bodies in the brain/SEG of *M. sexta*, and we have described in detail the branching patterns and projections of some of these neurons. OAir fibers were observed in most regions of the brain, and therefore it is likely that OA is involved

in many aspects of central processing in this moth. Wherever possible, we have compared our findings with the reported structural characteristics of OAir neurons in other insects. These comparisons, however, are strictly morphological in nature and do not suggest functions of OA in the brain of *M. sexta*.

We observed a large number of OAir cell bodies in the SEG of *M. sexta*. All nine OAir VUM1b neurons in the SEG were located in the labial neuromere. In addition, there were two ventral and medial (VS) OAir neurons in the maxillary neuromere of the SEG and a large number of OA-ir cell bodies located on the dorsal midline of the SEG which we believe are most likely DUM neurons. The number of OAir neurons observed on the dorsal midline of the SEG of *M. sexta* was similar to the number reported for *Locusta migratoria* (Bräunig, 1991; Stevenson et al., 1992), *Gryllus bimaculatus* (Spöhrhase-Eichmann et al., 1992), and *Periplaneta americana* (Eckert et al., 1992). The processes of the DS neurons in *M. sexta* have projections similar to those of locust metathoracic ganglion DUM neurons (Watson, 1984). DUM neurons of the locust metathoracic ganglion also have processes that either extend into the ganglion and then back to the dorsal surface (as was observed for *M. sexta* DS neurons; Fig. 8b) along the deep DUM tract or remain on the dorsal side of the ganglion and follow the superficial DUM tract (as was also observed for *M. sexta* DS neurons in the SEG) before bifurcating (Watson, 1984). Similar projection patterns have been described for DUM neurons in several other insects (Campbell et al., 1995; Bräunig 1997; Stevenson and Meuser, 1997). For excellent reviews on unpaired median neurons in insects, see Stevensen and Spöhrhase-Eichmann (1995) or Bräunig and Pflüger (2001).

In the locust SEG, the projection patterns of the DUM neurons were described in detail by Bräunig (1991). He suggested that these neurons contain OA because the number of OAir neurons in the dorsal region of the locust SEG and the number of DUM neurons was similar (Bräunig, 1991). Of the DUM neurons described in the locust, one in particular, DUM SA5, projects directly and primarily to the antennal lobes and another, DUM SA4, projects to both the antennal lobes and the mushroom bodies (Bräunig, 1991). It is therefore possible that the neurites projecting into the antennal lobe in *M. sexta* are produced by DUM neurons similar to DUM SA4 and SA5 in the locust, but we cannot rule out that these neurites are produced by VUM1b2 or by the VS neurons.

Of the nine VUM1b neurons, VUM1b3-9 project posteriorly through the ventral nerve cord. The targets of these neurons are currently being examined. The remaining two VUM1b neurons project dorsally toward the brain. The VUM1b1 neuron projects dorsally and arborizes extensively on the surface of the  $\gamma$ -lobes of the mushroom bodies and in the dorsal protocerebrum, where it branches both laterally and posteriorly. It is particularly noteworthy that VUM1b1 has extensive connections to the  $\gamma$ -lobes, as this is a region of the insect brain that has been implicated in short-term memory in *D. melanogaster* (Zars et al., 2000).

In addition to the OAir structures in the SEG described above, there are also two processes that enter the SEG from the ventral nerve cord and are mirror-image projections that cross the SEG midline (Fig. 10). The two fibers that together form the bilateral bridge branch in a very characteristic, bilaterally symmetric pattern in the SEG neuropil. These fibers may originate in a thoracic ganglion or possibly one of the abdominal ganglia, and therefore may convey either gustatory or mechanosensory information between the thorax or abdomen and the SEG.

### Comparisons of structures in *M. sexta* with other insect species

The distribution and anatomical features of OAir neurons in the brains of several insect species have been described. Kreissl et al. (1994) used a polyclonal antibody to examine the distribution of OAir neurons in the honey bee brain, and subsequent studies in the locust (Stern et al., 1995), the fruit fly (Monastiriotti et al., 1995), and *M. sexta* (this study) found similar neural



morphologies. *M. sexta* possesses OAir fibers with projection patterns similar to the anatomical descriptions of VUMmx1 in the honey bee (Hammer, 1993) which is thought to be octopaminergic (Kriessl et al., 1994; Hammer and Menzel, 1998; Menzel et al., 1999). The cell body of VUMmx1 is in a location similar to that of the OAir VUM neurons described by Kriessl et al. (1994), and all of the areas of the brain innervated by VUMmx1 (the ALs, mushroom bodies, and lateral protocerebrum) contain OAir fibers. In addition, the honey bee antennal lobe is innervated by OAir fibers that enter via the lateral antenno-glomerular tract; the same tract through which VUMmx1 innervates the antennal lobe. While the neurites in *M. sexta* that connect the ALs and the calyces of the mushroom bodies project to regions similar to VUMmx1 in the honey bee, there are major differences that suggest that these neurons may not be homologous in bees and moths. For example, VUMmx1 projects to the calyces via the lateral antenno-glomerular tract (Hammer, 1993), the equivalent of the outer antennal cerebral tract in *M. sexta*, while the OAir fibers in *M. sexta* that connect the calyces and the ALs project through the inner antenno-cerebral tract (IACT; the equivalent of the medial antenno-glomerular tract in the honey bee). Furthermore, because these fibers travel via the IACT, they do not first innervate the lateral protocerebrum and then proceed to the mushroom bodies, as is the case with VUMmx1 (Hammer, 1993). Moreover, we did not observe any OAir fibers that travel along the IACT enter the lateral protocerebrum.

In addition to OAir VUM neurons, there are other OAir structures in the brain of *M. sexta* that bear some similarity to those produced by specific OAir structures in several insect species. *Apis mellifera* (Kriessl et al., 1994; Sinakevitch et al., 2001), *L. migratoria* (Stern et al., 1995), *P. americana* (Sinakevitch et al., 2001), *Phaenicia sericata* (Sinakevitch et al., 2001) and *D. melanogaster* (Monastirioti et al., 1995; Sinakevitch et al., 2001) all have clusters of OAir PM neurons that are situated on either side of the esophageal foramen and that project posteriorly, then laterally towards the optic lobes. The OAir PM neurons have been most extensively studied in the locust, where they have been shown to contain OA (Stern et al., 1995) and to be involved in the dishabituation of the responses of movement detectors in the optic lobes to various visual stimuli (O'Shea and Rowell, 1975; Gauglitz and Stevenson, 1993; Bacon et al., 1995; Stern et al., 1995; Stern, 1998).

### Behavioral studies of octopamine in moths

In recent years, several studies have examined the effects of OA on the behavior of moths. Injection of OA into the hemolymph increases the sensitivity of male moths to the conspecific female's sex pheromone in both *Trichoplusia ni* and *Lymantria dispar* (Linn and Roelofs, 1986; Linn et al., 1992). In addition, OA has a time dependent effect on sensitivity of male *L. dispar* to sex pheromone. If OA is injected during photophase, there is no significant change (compared to controls) in the percentage of males that make contact with the sex-pheromone source. By contrast, if OA is injected just prior to scotophase, there is a significant increase in the percentage of males that contact the source when tested both during scotophase and in the subsequent photophase (Linn et al., 1992). Although it seems likely that injected OA affects peripheral structures such as the olfactory receptor cells or associated accessory cells (Pophof, 2000; Dolzer et al., 2001; Grosmaître et al., 2001; Pophof, 2002; Stelinski et al., 2003), injected OA does enter the central nervous system of *T. ni* (Linn et al., 1994) and has been shown to affect not only central motor centers involved in controlling flight (Claassen and Kammer, 1986), but also the activity of moth flight muscles (Fitch and Kammer, 1986; Klaassen et al., 1986). Changes in olfactory-guided flight behavior following OA injection are therefore probably due to a combination of central and peripheral effects.

In conclusion, based on the widespread distribution of OAir in the brain and SEG of *M. sexta*, we believe that OA must play a number of important roles in modulating patterns of neural activity in this insect. We have characterized a number of OAir neurons and branching

patterns that are anatomically similar to those described in other insects. In addition we have described some structures that have no known counterpart in other species.

Electrophysiological and pharmacological analysis of these cells and their connections are needed to determine if comparable functional homologies exist among species. In any case, our data provide additional evidence that complex networks of octopaminergic neurons are ubiquitous in insect nervous systems.

#### Acknowledgments

The authors thank Dr. A.A. Osman and Suzanne Mackzum for rearing of insects, H. Stein and P. Jansma for technical assistance, and Drs. N.T. Davis and L.A. Oland for invaluable discussions. We also thank Drs. N.T. Davis and H.-J. Pflöger for helpful comments on the manuscript. In addition, the authors thank Dr. I. Sinakevitch for hours of very helpful technical assistance. This work was supported by grants from the National Institute on Deafness and Other Communication Disorders, DC-05652 (to TAC) and DC-02751 (to JGH), and an award from the National Science and Engineering Research Council of Canada PGS B-244345-2003 (to AMD).

#### List of Abbreviations:

AL, antennal lobe; DP, dorsal protocerebrum; DS, dorsal subesophageal ganglion; EF, esophageal foramen; OA, octopamine; OA<sub>ir</sub>, octopamine-like immunoreactivity; PM, protocerebral medulla; SEG, subesophageal ganglion; VNC, ventral nerve cord; VUM, ventral unpaired median.

#### References:

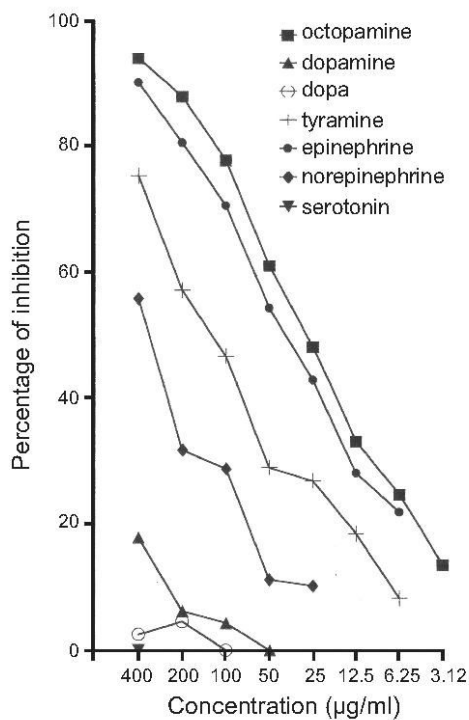
- Bacon JP, Thompson KSJ, Stern M. Identified octopaminergic neurons provide an arousal mechanism in the locust brain. *J Neurophysiol* 1995;74:2739–2743. [PubMed: 8747228]
- Bell RA, Joachim FA. Techniques for rearing laboratory colonies of tobacco hornworm and pink bollworms. *Ann Ent Soc Am* 1996;69:365–373.
- Bräunig P. Subesophageal DUM neurons in the principal neuropiles of the locust brain. *Phil Trans Royal Soc London B* 1991;332:221–240.
- Bräunig P. The peripheral branching pattern of identified dorsal unpaired median (DUM) neurons in the locust. *Cell Tiss Res* 1997;290:641–654.
- Bräunig P, Pflüger HJ. The unpaired median neurons of insects. *Adv Insect Physiol* 2001;28:185–266.
- Campbell HR, Thompson KJ, Siegler MVS. Neurons of the median neuroblast lineage of the grasshopper: A population study of the efferent DUM neurons. *J Comp Neurol* 1995;358:541–551. [PubMed: 7593748]
- Christensen TA, Hildebrand JG. Male-specific, sex-pheromone-selective projection neurons in the antennal lobes of the moth *Manduca sexta*. *J Comp Physiol A* 1987;160:553–569. [PubMed: 3612589]
- Christensen TA, Sherman TG, McCaman RE, Carlson AD. Presence of octopamine in firefly photomotor neurons. *Neurosci* 1983;9(1):183–189.
- Claassen DE, Kammer AE. Effects of octopamine, dopamine and serotonin on production of flight motor output by thoracic ganglia of *Manduca sexta*. *J Neurobiol* 1986;17:1–14. [PubMed: 3088211]
- Cunningham JP, Moore CJ, Zalucki MP, West SA. Learning, odour preference and flower foraging in moths. *J Comp Physiol A* 2004;207:87–94.
- Daly KC, Chandra S, Durtschi ML, Smith BH. The generalization of an olfactory-based conditioned response reveals unique but overlapping odour representations in the moth *Manduca sexta*. *J Exp Biol* 2001a;204:3085–3095. [PubMed: 11551996]
- Daly KC, Christensen TA, Lei H, Smith BH, Hildebrand JG. Learning modulates the ensemble representations for odors in primary olfactory networks. *Proc Natl Acad Sci USA* 2004;101(28):10476–10481. [PubMed: 15232007]
- Daly KC, Durtschi ML, Smith BH. Olfactory-based discrimination learning in the moth, *Manduca sexta*. *J Insect Physiol* 2001b;47:375–384. [PubMed: 11166302]
- Daly KC, Smith BH. Associative olfactory learning in the moth *Manduca sexta*. *J Exp Biol* 2000;203:2025–2038. [PubMed: 10851119]

- Davenport AP, Evans PD. Stress-induced changes in the octopamine levels of insect haemolymph. *Insect Biochem* 1984;14:135–143.
- Davenport AP, Wright DJ. Octopamine distribution in the larvae and adults of the two species of moth *Spodoptera littoralis* and *Manduca sexta*. *J Insect Physiol* 1986;32:987–993.
- Davis NT, Homberg U, Teal PE, Altstein M, Agricola HJ, Hildebrand JG. Neuroanatomy and immunocytochemistry of the median neuroendocrine cells of the subesophageal ganglion of the tobacco hawkmoth, *Manduca sexta*: immunoreactivities to PBAN and other neuropeptides. *Microsc Res Tech* 1996;35:201–229. [PubMed: 8956271]
- Dolzer J, Krannich S, Fischer K, Stengl M. Oscillations of the transepithelial potential of moth olfactory sensilla are influenced by octopamine and serotonin. *J Exp Biol* 2001;204:2781–2794. [PubMed: 11683434]
- Donini A, Agricola HJ, Lange AB. Crustacean cardioactive peptide is a modulator of oviduct contractions in *Locusta migratoria*. *J Insect Physiol* 2001;47:277–285. [PubMed: 11119773]
- Dudai Y, Buxbaum J, Corfas M. Foramidines interact with *Drosophila* octopamine receptors, alter the flies' behavior and reduce their learning ability. *J Comp Physiol A* 1987;161:739–746.
- Eckert M, Rapus J, Nurnberger A, Penzlin H. A new specific antibody reveals octopamine-like immunoreactivity in cockroach ventral nerve cord. *J Comp Neurol* 1992;322:1–15. [PubMed: 1430305]
- Essig, U. Monoklonale Antikörper. Herstellung und Charakterisierung. Peters JH. Baumgarten H. Springer Verlag; Berlin: 1990. Subklassentypisierung von Antikörpern der Maus mittels ELISA; p. 415-420.
- Evans PD. Biogenic amines in the insect nervous system. *Adv Insect Physiol* 1980;15:317–474.
- Fan RJ, Anderson P, Hansson B. Behavioural analysis of olfactory conditioning in the moth *Spodoptera littoralis* (Boisd.) (Lepidoptera: Noctuidae). *J Exp Biol* 1997;200:2969–2976. [PubMed: 9359884]
- Fan RJ, Hansson BS. Olfactory discrimination conditioning in the moth *Spodoptera littoralis*. *Physiol Behav* 2001;72:159–165. [PubMed: 11239993]
- Farooqui T, Robinson K, Vaessin H, Smith BH. Modulation of early olfactory processing by an octopaminergic reinforcement pathway in the honeybee. *J Neurosci* 2003;23:5370–5380. [PubMed: 12832563]
- Fitch GK, Kammer AE. Effects of octopamine and forskolin on excitatory junction potentials of developing and adult moth *Manduca sexta* muscle. *J Neurobiol* 1986;17:303–316. [PubMed: 3018149]
- Gauglitz, S.; Stevensen, P. Gene-brain-behavior. Elsner H. Heisenberg M. Thieme; New York: 1993. Octopamine enhances responsiveness of a locust movement detector interneurone (DCMD); p. 608
- Grosmaître X, Marion-Poll F, Renou M. Biogenic amines modulate olfactory receptor neurons firing activity in *Mamestra brassicae*. *Chem Senses* 2001;26:653–661. [PubMed: 11473931]
- Hammer M. An unidentified neuron mediates the unconditioned stimulus in associative olfactory learning in honeybees. *Nature* 1993;366:59–63.
- Hammer M, Menzel R. Learning and memory in the honeybee. *J Neurosci* 1995;3:1617–1630. [PubMed: 7891123]
- Hammer M, Menzel R. Multiple sites of associative odor learning as revealed by local brain microinjections of octopamine in honeybees. *Learn Mem* 1998;5:146–156. [PubMed: 10454379]
- Harlow, E.; Lane, D. Cold Spring Harbor Lab; New York: 1988. Antibodies. A laboratory manual.
- Hartlieb E. Olfactory conditioning in the moth *Heliothis virescens*. *Naturwissenschaften* 1996;83:87–88.
- Hartlieb E, Anderson P, Hansson BS. Appetitive learning of odours with different behavioural meaning in moths. *Physiol Behav* 1999;67:671–677. [PubMed: 10604836]
- Hildebrand H, Müller U. Octopamine mediates rapid stimulation of protein kinase A in the antennal lobe of honeybees. *J Neurobiol* 1995;27:44–50. [PubMed: 7643074]
- Homberg, U. Stuttgart; Jena. Rathmayer W. Gustav Fischer; New York: 1994. Distribution of neurotransmitters in the insect brain. *Prog Zool* 40.
- Homberg U, Hildebrand JG. Serotonin-immunoreactive neurons in the median protocerebrum and subesophageal ganglion of the sphinx moth *Manduca sexta*. *Cell Tiss Res* 1989;258:1–24.

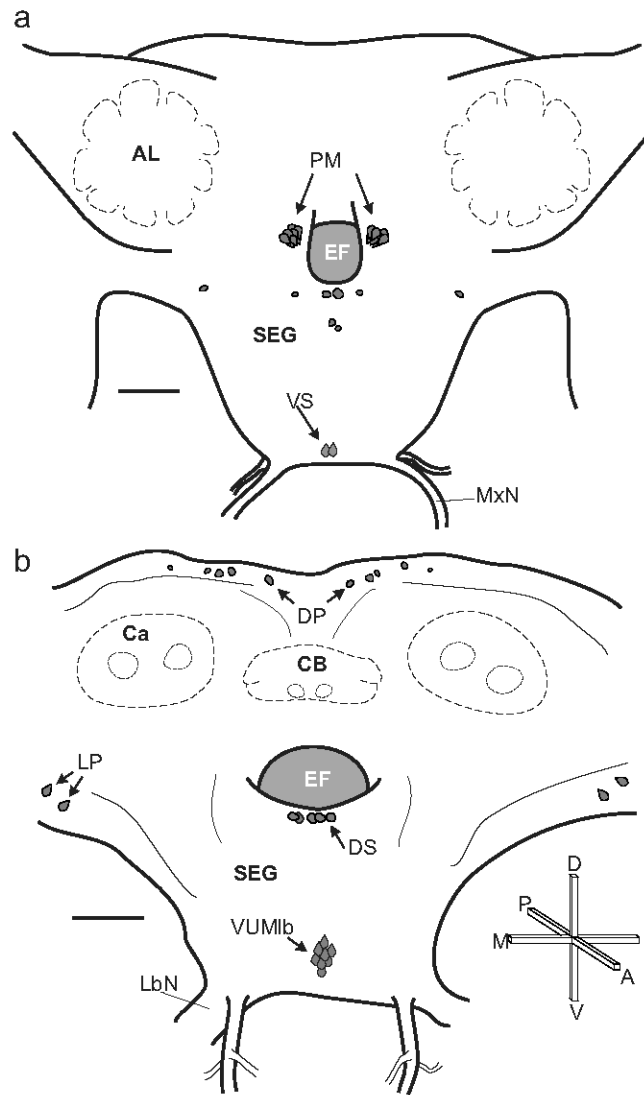
- Homberg U, Montague RA, Hildebrand JG. Anatomy of antenno-cerebral pathways in the brain of the sphinx moth *Manduca sexta*. *Cell Tiss Res* 1988;254:255–281.
- Hoyle G. Evidence that insect dorsal unpaired median (DUM) neurons are octopaminergic. *J Exp Zool* 1975;193:433–439. [PubMed: 1100767]
- Karsten U, Rudolph M. Monoclonal antibodies against tumor-associated antigens: Mycoplasma as a major technical obstacle and its possible circumvention by azaserine selection medium. *Archiv Geschwulstforschung* 1985;55:305–310.
- Kearny JF, Radbruch A, Liesegang B, Rajewski K. A new mouse myeloma cell line that has lost immunoglobulin expression but permits the construction of antibody-secreting hybrid cell lines. *J Immunol* 1979;123:1548–1550. [PubMed: 113458]
- Klaassen LW, Kammer AE, Fitch GK. Effects of octopamine on miniature junction potentials from developing and adult moth *Manduca sexta* muscle. *J Neurobiol* 1986;17:291–302. [PubMed: 3018148]
- Kreissl S, Eichmüller S, Bicker G, Rapus J, Eckert M. Octopamine-like immunoreactivity in the brain and subesophageal ganglion of the honeybee. *J Comp Neurol* 1994;348:583–595. [PubMed: 7530730]
- Lehman HE, Klukas KA, Gilchrist LS, Mesce KA. Steroid regulation of octopamine expression during metamorphic development of the moth *Manduca sexta*. *J Comp Neurol* 2000a;424:283–296. [PubMed: 10906703]
- Lehman HK, Murgiu C, Hildebrand JG. Characterization and development regulation of tyramine- $\beta$ -hydroxylase in the CNS of the moth *Manduca sexta*. *Insect Biochem Mol Biol* 2000b;30:377–386. [PubMed: 10745161]
- Linn CE, Campbell MG, Roelofs WL. Photoperiod cues and the modulatory action of octopamine and 5-hydroxytryptamine on locomotor and pheromone response in male gypsy moths, *Lymantria dispar*. *Arch Insect Biochem Physiol* 1992;20:265–284.
- Linn CE Jr, Poole KR, Roelofs WL. Studies on biogenic amines and their metabolites in nervous tissue and hemolymph of adult cabbage looper moths: III. Fate of injected octopamine, 5-hydroxytryptamine, and dopamine. *Comp Biochem Physiol* 1994;108C:99–106.
- Linn CE, Roelofs WL. Modulatory effects of octopamine and serotonin on male sensitivity and periodicity of response to sex pheromone in the cabbage looper moth, *Trichoplusia ni*. *Arch Insect Biochem Physiol* 1986;3:161–171.
- Maxwell GD, Tait JF, Hildebrand JG. Regional synthesis of neurotransmitter candidates in the CNS of the moth *Manduca sexta*. *Comp Biochem Physiol* 1978;61C:109–119.
- Mercer A, Menzel R. The effects of biogenic amines on conditioned and unconditioned responses to olfactory stimuli in the honeybee *Apis mellifera*. *J Comp Physiol* 1982;145A:363–368.
- Menzel R, Heyne A, Kinzel C, Gerber B, Fiala A. Pharmacological dissociation between the reinforcing, sensitizing, and response-releasing functions of reward in honeybee classical conditioning. *Behav Neurosci* 1999;113:744–754. [PubMed: 10495082]
- Monastirioti M, Gorczyca M, Rapus J, Eckert M, White K, Budnick V. Octopamine immunoreactivity in the fruit fly *Drosophila melanogaster*. *J Comp Neurol* 1995;356:275–287. [PubMed: 7629319]
- Muller, S. Peptide carrier conjugation. Techniques in biochemistry and molecular biology. In: Burdon, RH.; van Knippenberg, PH., editors. Synthetic polypeptides as antigens. 19. Elsevier; Amsterdam: 1988. p. 95-130.
- Murphy, JF.; Davies, DH.; Smith, CJ. The development of enzyme-linked immunosorbent assays (ELISA) for catecholamines as antigens. In: Burdon, RH.; van, Knippenberg PH., editors. Laboratory techniques in biochemistry and molecular biology. 19. Elsevier; Amsterdam: 1992. p. 95-130.
- Orchard I, Lange A. Cyclic AMP in locust fat body: correlation with octopamine and adipokinetic hormones during flight. *J. Insect Physiol* 1984;30:901–904.
- O'Shea M, Rowell CHF. A spike-transmitting electrical synapse between visual interneurons in the locust movement detector system. *J Comp Physiol* 1975;97:143–158.
- Pflüger HJ, Witten JL, Levine RB. Fate of abdominal ventral unpaired median cells during metamorphosis of the hawkmoth, *Manduca sexta*. *J Comp Neurol* 335:508–522. [PubMed: 8227533]
- Pophof B. Octopamine modulates the sensitivity of silkworm pheromone receptor neurons. *J Comp Physiol A* 2000;186:307–313. [PubMed: 10757246]

- Pophof B. Octopamine enhances moth olfactory responses to pheromones, but not those to general odorants. *J Comp Neurol* 2002;188:659–662.
- Roeder T. Octopamine in invertebrates. *Prog Neurobiol* 1999;59:533–561. [PubMed: 10515667]
- Schwaerzel M, Monastirioti M, Scholz H, Friggi-Grelin F, Birman S, Heisenberg M. Dopamine and octopamine differentiate between aversive and appetitive olfactory memories in *Drosophila*. *J Neurosci* 2003;23:10495–10502. [PubMed: 14627633]
- Sinakevitch, I.; Niwa, M.; Strausfeld, N. Soc Neurosci Abstract. 2001. Octopamine immunoreactivity reveals homologous organization in the optic lobes and brain of the fly, honey bee and cockroach; p. 518-19.
- Spörhase-Eichmann U, Vullings HG, Buijs RM, Horn21wer M, Schurmann FW. Octopamine-immunoreactive neurons in the central nervous system of the cricket, *Gryllus bimaculatus*. *Cell Tiss Res* 1992;268:287–304.
- Stern M, Thompson KS, Zhou P, Watson DG, Midgley JM, Gewecke M, Bacon JP. Octopaminergic neurons in the locust brain: morphological, biochemical, and electrophysiological characterization of potential modulators of the visual system. *J Comp Physiol* 1995;177:611–625.
- Stern M. Octopamine in the locust brain: Cellular distribution and functional significance in an arousal mechanism. *Microsc Res Tech* 1999;45:135–141. [PubMed: 10344765]
- Stelinski LL, Miller JR, Ressa NE, Gut LJ. Increased EAG responses of tortricid moths after prolonged exposure to plant volatiles: evidence for octopaminemediated sensitization. *J Insect Physiol* 2003;49:845–856. [PubMed: 16256687]
- Stevenson PA, Meuser S. Octopaminergic innervation and modulation of a locust flight steering muscle. *J Exp Biol* 1997;200:633–642. [PubMed: 9318358]
- Stevenson PA, Pfluger HJ, Eckert M, Rapus J. Octopamine immunoreactive cell populations in the locust thoracic-abdominal nervous system. *J Comp Neurol* 1992;315:382–397. [PubMed: 1373157]
- Stevenson PA, Spörhase-Eichmann U. Localization of octopaminergic neurones in insects. *Comp Biochem Physiol A* 1995;110:203–215.
- Strausfeld, N. Atlas of an insect brain. Springer-Verlag; Berlin; New York: 1976.
- Watson AHD. The dorsal unpaired median neurons of the locust metathoracic ganglion: neuronal structure and diversity, and synapse distribution. *J Neurocytol* 1984;13:303–327. [PubMed: 6726291]
- Zars T, Fischer M, Schulz R, Heisenberg M. Localization of a short-term memory in *Drosophila*. *Science* 2000;288:672–675. [PubMed: 10784450]

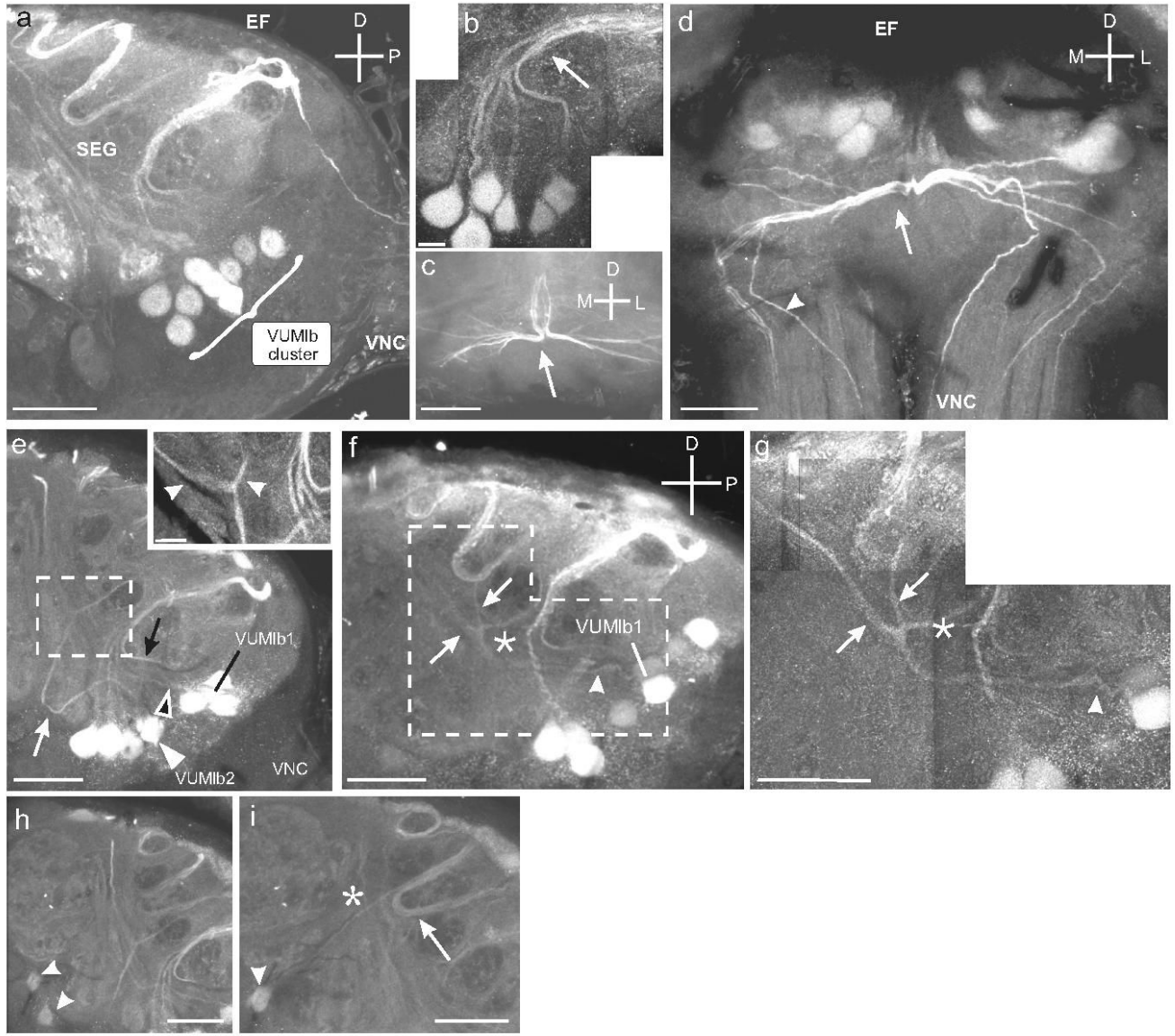




**Fig. 1.** Cross-reactivity of the OA-antiserum with other biogenic amines was determined with enzyme-linked immunosorbent assay (ELISA). The percent inhibition (ordinate) of binding of OA-antibody is shown in relation to the concentration (abscissa) of the tested amines. The test shows no or low cross-reaction with serotonin, DOPA and dopamine. In contrast, the activity of the MAb-OA1 is inhibited by epinephrine and less so by tyramine and norepinephrine.



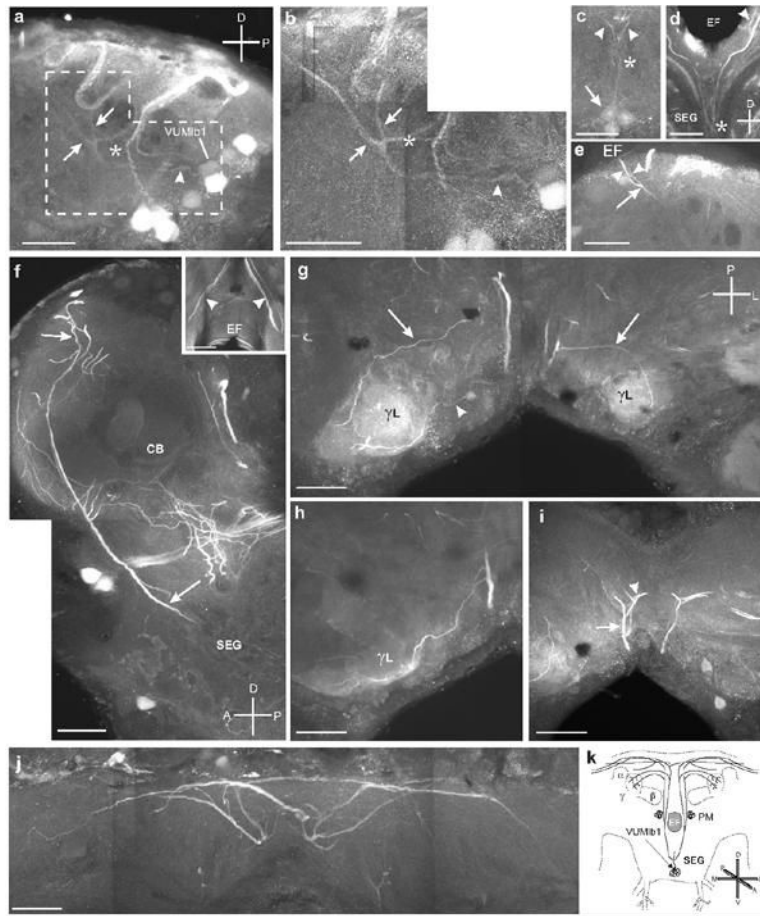
**Fig. 2.** Distribution of OAir cell bodies in the brain and SEG of adult *M. sexta*. **a.** Frontal view of the anterior portion of the brain (adapted from Homberg et al., 1988). Several of the key cell groups are labeled: two ventral SEG (VS) neurons in the maxillary neuromere, and more dorsally, the bilateral clusters of protocerebral medulla cells (PM) are shown on either side of the esophageal foramen (EF). Also shown are two pairs of dorsal midline cells and two bilateral cell pairs, one of which sits ventro-laterally to the antennal lobes (AL). **b.** Frontal view of the posterior portion of the brain and SEG (adapted from Homberg and Hildebrand, 1989). Shown in this view is the cluster of mVUM neurons in the labial neuromere, the dorsal SEG (DS) cells, the lateral protocerebral (LP) cells, and the dorsal protocerebral (DP) cells situated above the mushroom body calyces (Ca) and the central body (CB). Scale bars = 200  $\mu\text{m}$ . Crossbars show the orientation of the brain, indicating the posterior (P), anterior, (A), dorsal (D), ventral (V), lateral (L) and medial (M) directions. The same conventions and abbreviations are used for all figures.



**Fig. 3.**

Details of the VUMlb cluster and the projections cells in the cluster. **a.** Sagittal section through the SEG shows the VUMlb (9 cells) situated in the posterior SEG. **b.** Higher magnification montage of VUMlb neurons projecting dorsally and then posteriorly in a tight bundle (arrow). **c.** Horizontal section through the dorso-posterior portion of the SEG shows the divergence of the bundle of VUMlb neurites (arrow). **d.** Frontal section through the SEG shows the diverging bundle and the bilateral projections through the VNC (arrowheads). **e.** Sagittal section through the SEG showing the VUMlb2 neurites projecting anteriorly before turning dorsally. VUMlb2 (white arrowhead) loops anteriorly before turning dorsally (white arrow). VUMlb1 also projects anteriorly (black arrowhead; see Fig. 4) and then dorsally (black arrow). Inset shows the first branch point of VUMlb2 as it bifurcates below the EF (arrowheads). **f.** Sagittal section through the SEG shows the neurite of VUMlb1 as it projects anteriorly (arrowhead) and then bifurcates. Inset shows the neurite as it divides, giving rise to bilateral projections traveling dorsally (arrowheads). **g.** Montage of sagittal section through the SEG shows the two faintly labeled VS neurons (arrowheads). **h.** Sagittal section through the SEG shows the projection

(arrow) of one of the VS neurons (arrowhead) as it extends dorsally and posteriorly, parallel to the neurites of the dorsal SEG (DS; Fig. 7) neurons (asterisk). Scale bars = 50  $\mu\text{m}$  in **a**, **c**, **d**, **g-i** and 12.5  $\mu\text{m}$  in **b**, **e**, **f**.

**Fig. 4.**

**a.** Sagittal section through the SEG shows VUM1b1 sending a projection anteriorly (arrowhead), which then bifurcates (arrows). The paired parallel processes then continue dorsally. Dashed outline indicates the area highlighted in **b**. **b.** Montage of sagittal section through the SEG shows the primary neurite (arrowhead) of VUM1b2 and its branching pattern in the SEG, including the two antero-dorsal projections (arrows) and the single posterior projection (asterisk). **c.** Frontal section through the ventral portion of the SEG shows VUM1b1 (arrowhead) as it bifurcates (asterisk) along the lateral axis and projects dorsally (arrowheads). **d.** Frontal section showing the bifurcation (asterisk) of the primary neurites of the VUM1b1 neuron and the two branches traveling dorsally up out of the SEG into the tritocerebrum (arrowheads). **e.** Sagittal section showing the ascending process of the VUM1b1 neuron as it bifurcates just below the EF (arrow) in the anterior portion of the SEG and sends two branches dorsally (arrowheads). **f.** Montage of sagittal section shows two fibers (one thick, one thinner) projecting dorsally from the SEG to the dorso-anterior portion of the protocerebrum (arrows). This projection passes between the cluster of PM neurons (see below) and the EF. Inset shows a frontal section through the protocerebrum demonstrating that there are at least two branches that extend dorsally on either side of the EF. **g.** Montage of a horizontal section through the protocerebrum shows fine arborizations projecting to and arborizing in the  $\gamma$ lobes ( $\gamma$ L) of the ipsilateral mushroom body. The projections reach  $\gamma$ L from both an anterior (arrowhead) and a posterior (arrow) trajectory. **h.** Horizontal section shows that the fine arborizations in  $\gamma$ L appear to be restricted to the surface (note the lack of staining inside lobe). **i.** Horizontal section shows the projections (arrow) as they continue dorsally and then branch (arrowhead). **j.** Montage of a frontal section shows the extensive bilateral projections (arrows) of VUM1b1 in the dorsal



protocerebrum. Scale bars = 50  $\mu\text{m}$ . **k.** Illustration of the projections of VUM1b1 throughout the brain.

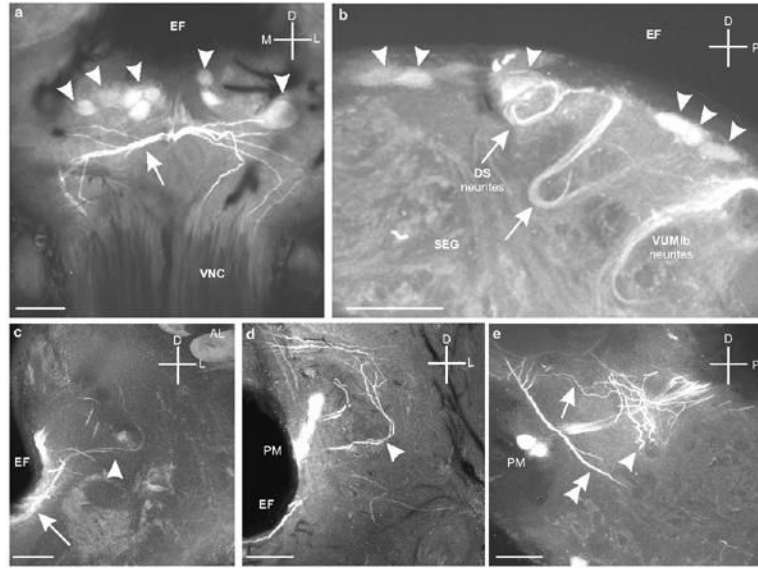


**Fig. 5.**

**a.** Frontal section through the SEG shows the dorsal SEG (DS) cells (arrowheads) below the esophageal foramen (EF) and above the branches produced by the VUM1b neurons (arrow) that project down the VNC (Fig. 2d). **b.** Sagittal section through the SEG shows the primary neurites of the DS cells (arrowheads) as they loop ventrally and then turn back dorsally (arrows). **c.** Frontal section through the tritocerebrum shows the projections of the DS neurons extending laterally along the ventral side of the EF (arrow) and then branching in the tritocerebrum (arrowhead) below the antennal lobe (AL). **d.** Frontal section through the tritocerebrum shows some of the branches of the DS neurons (arrowhead) that extend above the PM neurons. **e.** Sagittal section (detail from Figure 4f) showing the thicker branches of DS neurons as they spread out into both the dorsal (arrow) and ventral (arrowhead) regions of the tritocerebrum. The major ascending processes of VUM1b1 are also clearly visible (double arrowhead). Scale bars = 50  $\mu\text{m}$ .

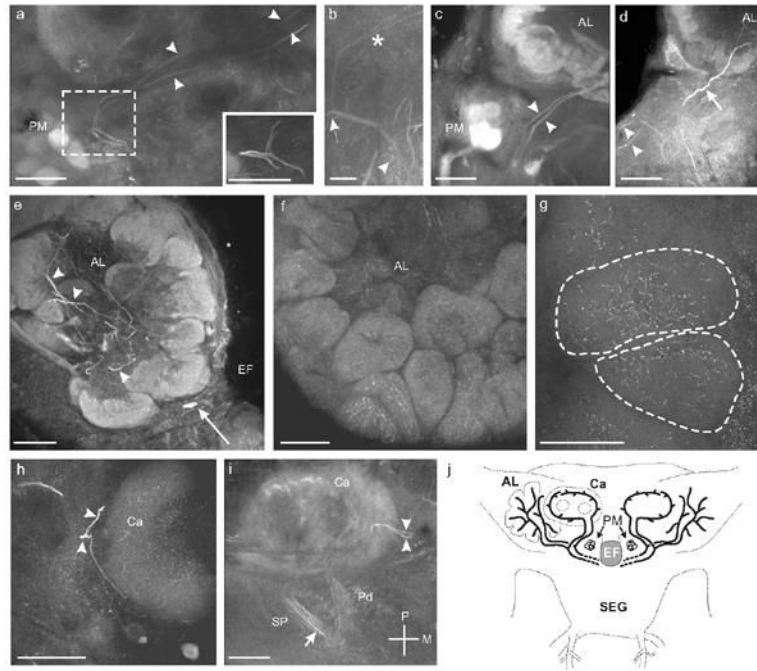


**Fig. 6.**

**a.** Sagittal section through the right midbrain showing one branch from each process traveling anteriorly to innervate the AL while the other branch travels dorsally and posteriorly (arrowheads) to innervate the mushroom bodies. Inset shows a higher magnification view of the bifurcation of the two processes before they enter the ALs. **b.** Sagittal section through the midbrain showing the branches originating from the ventral surface of the esophageal foramen (arrowhead) before bifurcating (arrow) and sending branches anteriorly and posteriorly (asterisk). Scale bar = 12.5  $\mu\text{m}$ . **c.** Frontal section shows the two processes (arrowheads) entering the ipsilateral antennal lobe (AL). **d.** Frontal section shows a third process (arrow) entering the AL anterior to the processes from in **a-c** (arrowheads). **e.** Frontal section shows numerous branched processes in the coarse neuropil of the AL (arrowheads). A single OAir cell body that sits ventromedial to the AL in the tritocerebrum is also visible (arrow; Fig. 1a). **f.** Frontal section through the AL reveals fine OAir arborizations in all AL glomeruli. **g.** Frontal section through the AL shows fine arborizations distributed throughout two glomeruli (dashed outlines). **h.** Sagittal section through the calyx (Ca) of the ipsilateral mushroom body shows one process branching and entering at the basal ring (arrowheads). **i.** Oblique horizontal section through the left mushroom body shows the two processes (arrowheads) innervating Ca at the basal ring. OAir processes are also visible in the primary pedunculus (Pd) and the secondary pedunculus (SP) (arrows). Scale bars = 50  $\mu\text{m}$  **a, c-i** and 12.5  $\mu\text{m}$  in **b**. **j.** Summary illustration of the processes innervating the ALs and the MBs.

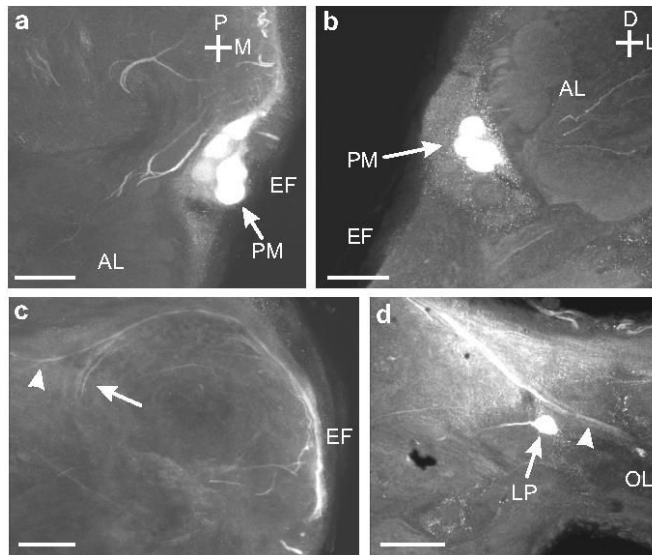


**Fig. 7.** **a.** Horizontal section through the EF showing the position of the OAir protocerebral medulla (PM) neurons (arrow). This cluster of cells lies posterior and medial to the AL. **b.** Frontal section through the anterior portion of the brain showing the position of the PM cell bodies (arrows) relative to the EF. **c.** Horizontal section through the EF shows the OAir projections of the PM neurons into the posterior portion of the brain, then laterally toward the optic lobe (arrowhead), or turning anteriorly in the protocerebrum (arrow). **d.** Processes (arrowhead) from PM neurons entering the optic lobe (OL). A single lateral protocerebral (LP) neuron is also visible (arrow). Scale bars = 50  $\mu$ m.

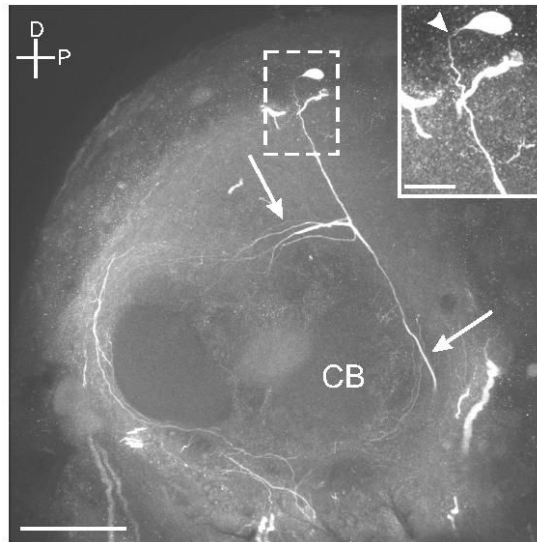


**Fig. 8.** Sagittal section through the protocerebrum shows a dorsal protocerebral neuron projecting ventrally and anteriorly (arrows) above the central body (CB). Scale bar = 50  $\mu\text{m}$ . Inset shows a higher magnification view of the cell body (arrowhead) confirming the origin of these projections. Scale bar = 12.5  $\mu\text{m}$ .



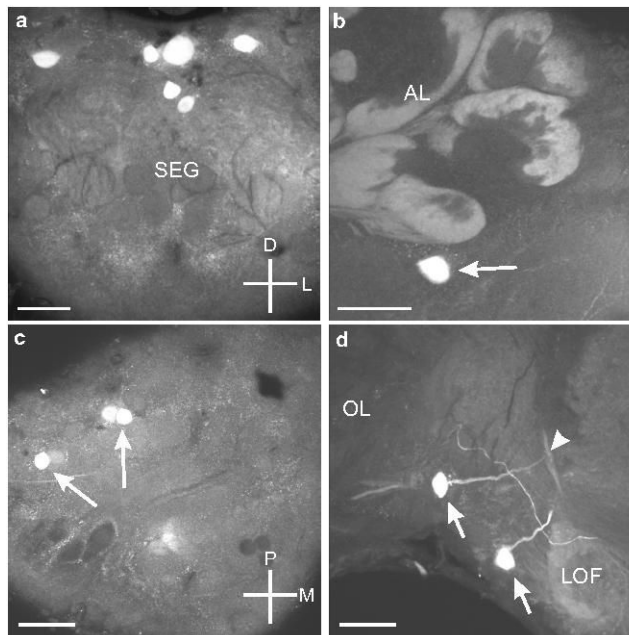


**Fig. 9.**  
**a.** Frontal section shows the six OAir cell bodies in the dorso-anterior portion of the SEG (see Fig. 1a). **b.** Frontal section through the tritocerebrum shows the single cell body that sits ventral to the AL (arrow). **c.** Horizontal section through the protocerebrum shows the three OA-ir cell bodies (arrows) in the dorso-posterior portion of the protocerebrum. **d.** Frontal section through the tritocerebrum and optic lobe of the left side of the brain shows the two OAir cell bodies (arrows) located dorso-laterally to the lateral optic foci (LOF) near the optic lobes (OL). One of the cells gives rise to a neurite that bifurcates above the LOF (arrowhead). Scale bars = 50  $\mu$ m.

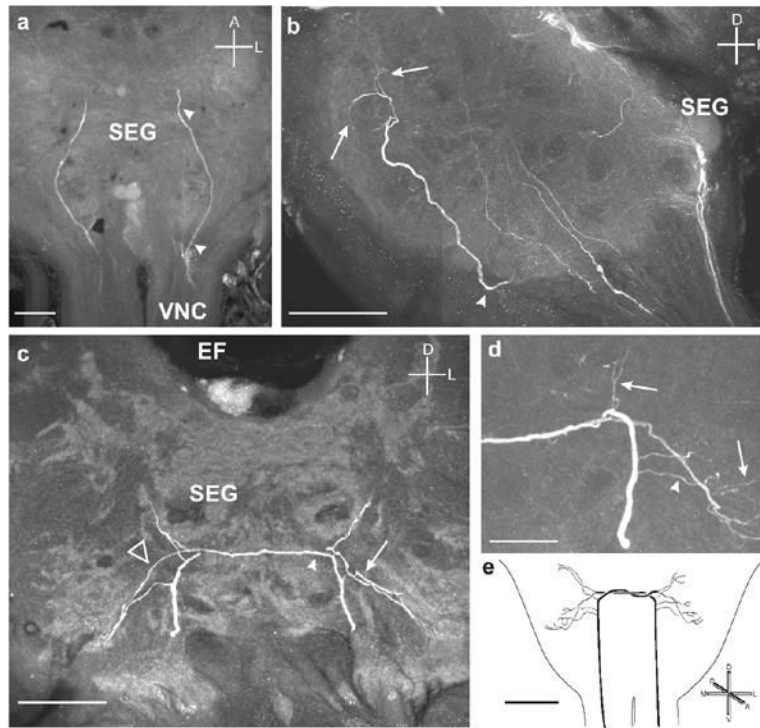


**Fig. 10.**

**a.** Horizontal section showing two branches entering the ventral portion of the SEG from each connective of the VNC and extending to the anterior margin of the SEG. **b.** Sagittal section showing one of the branches (arrowhead) projecting dorsally and producing fine arborizations (arrows) in the dorso-anterior portion of the SEG. **c.** Frontal section showing each process producing fine arborizations (arrow) and then projecting to the contralateral side of the SEG by following the branch of the other process (arrowhead). The processes then produce finer branches on the contralateral side (open triangle). **d.** Frontal section through the SEG shows the fine arbors produced by both the ipsilateral (arrowhead) and contralateral (arrows) branches entering the SEG from the VNC. **e.** Summary diagram of the ascending OAir fibers from the VNC that bilaterally innervate the SEG. Scale bars = 50  $\mu\text{m}$  in **a-c**, 25  $\mu\text{m}$  in **d**, and 200  $\mu\text{m}$  in **e**.